High-Reynolds-Number Asymptotics of Turbulent Boundary Layers: from Fully Attached to Marginally Separated Flows

Dedicated to Professor Klaus Gersten on the occasion of his 80th birthday

Alfred Kluwick and Bernhard Scheichl

Institute of Fluid Mechanics and Heat Transfer, Vienna University of Technology, Resselgasse 3/E322, A-1040 Vienna, Austria
alfred.kluwick@tuwien.ac.at, bernhard.scheichl@tuwien.ac.at

Summary. This paper reports on recent efforts with the ultimate goal to obtain a fully self-consistent picture of turbulent boundary layer separation. To this end, it is shown first how the classical theory of turbulent small-defect boundary layers can be generalised rigorously to boundary layers with a slightly larger, i.e. moderately large, velocity defect and, finally, to situations where the velocity defect is of $O(1)$. In the latter case, the formation of short recirculation zones describing marginally separated flows is found possible, as described in a rational manner.

Key words: marginal separation; perturbation methods; turbulent boundary layers
PACS: 40.10.A; 47.27.eb; 47.27.Jv; 47.27.nb; 47.32.Ff

1 Introduction

Despite the rapid increase of computer power in the recent past, the calculation of turbulent wall-bounded flows still represents an extremely challenging and sometimes insolvable task. Direct-Numerical-Simulation computations based on the full Navier–Stokes equations are feasible for moderately large Reynolds numbers only. Flows characterised by much higher Reynolds numbers can be investigated if one resorts to turbulence models for the small scales, as accomplished by the method of Large Eddy Simulation, or for all scales, as in computer codes designed to solve the Reynolds-averaged Navier–Stokes equations. Even then, however, the numerical efforts rapidly increase with increasing Reynolds number. This strongly contrasts the use of asymptotic theories, the performance of which improves as the values of the Reynolds number become larger and, therefore, may be considered to complement purely numerically based work.

With a few exceptions (e.g. [7,21]), studies dealing with the high-Reynolds-number properties of turbulent boundary layers start from the time- or, equivalently, Reynolds-averaged equations. By defining non-dimensional variables in terms of a representative length $\tilde{L}$ and flow speed $\tilde{U}$ and assuming incompressible nominally steady two-dimensional flow they take on the form

$$\frac{\partial u}{\partial x}+\frac{\partial v}{\partial y}=0\,, \tag{1a}$$

$$u\frac{\partial u}{\partial x}+v\frac{\partial u}{\partial y}=-\frac{\partial p}{\partial x}+\frac{1}{Re}\nabla^2 u-\frac{\partial\overline{u'^2}}{\partial x}-\frac{\partial\overline{u'v'}}{\partial y}\,, \tag{1b}$$

$$u\frac{\partial v}{\partial x}+v\frac{\partial v}{\partial y}=-\frac{\partial p}{\partial y}+\frac{1}{Re}\nabla^2 v-\frac{\partial\overline{u'v'}}{\partial x}-\frac{\partial\overline{v'^2}}{\partial y}\,. \tag{1c}$$

Herein $\nabla^2=\partial^2/\partial x^2+\partial^2/\partial y^2$, and (x,y), (u,v), $(u'v')$, $-\overline{u'^2}$, $-\overline{u'v'}$, $-\overline{v'^2}$, and p are Cartesian coordinates measuring the distance along and perpendicular to the wall, the corresponding time mean velocity components, the corresponding velocity fluctuations, the components of the Reynolds stress tensor, and the pressure, respectively. The Reynolds number is defined by $Re:=\tilde{U}\tilde{L}/\tilde{\nu}$, where $\tilde{\nu}$ is the (constant) kinematic viscosity. Equations (1) describe flows past flat walls. Effects of wall curvature can be incorporated without difficulty but are beyond the scope of the present analysis.

When it comes down to the solution of the simplified version of these equations provided by asymptotic theory in the limit $Re\to\infty$, one is, of course, again faced with the closure problem. The point, however, is that these equations and the underlying structure represent closure independent basic physical mechanisms characterising various flow regions identified by asymptotic reasoning. This has been shown first in the outstanding papers [5, 8, 10, 31], and more recently and in considerable more depth and breath, in [24,30] for the case of small-defect boundary layers, which will be considered in Sect. 2. Boundary layers exhibiting a slightly larger, i.e. a moderately large, velocity defect are treated in Sect. 3. Finally, Sect. 4 deals with situations where the velocity defect is of $O(1)$ rather than small.

2 Classical Theory of Turbulent Small-Defect Turbulent Boundary Layers

We first outline the basic ideas underlying an asymptotic description of turbulent boundary layers.

2.1 Preliminaries

Based on dimensional reasoning put forward by L. Prandtl and Th. von Kármán, a self-consistent time-mean description of firmly attached fully developed turbulent boundary layers holding in the limit of large Reynolds numbers Re, i.e.

for $Re \to \infty$, has been proposed first in the aforementioned studies [5,8,10,31]. One of the main goals of the present investigation is to show that this rational formulation can be derived from a minimum of assumptions:

(a) all the velocity fluctuations are of the same order of magnitude in the limit $Re \to \infty$, so that all Reynolds stress components are equally scaled by a single velocity scale u_{ref}, non-dimensional with a global reference velocity (hypothesis of locally isotropic turbulence);
(b) the pressure gradient does not enter the flow description of the viscous wall layer to leading order (assumption of firmly attached flow);
(c) the results for the outer predominantly inviscid flow region can be matched directly with those obtained for the viscous wall layer (assumption of "simplest possible" flow structure).

In the seminal studies [5, 8, 10, 31], u_{ref} is taken to be of the same order of magnitude in the fully turbulent main portion of the boundary layer and in the viscous wall layer and, hence, equal to the skin-friction velocity

$$u_\tau := \left[Re^{-1}(\partial u/\partial y)_{y=0}\right]^{1/2} \ . \tag{2}$$

This in turn leads to the classical picture, according to which (i) the streamwise velocity defect with respect to the external impressed flow is small and of $O(u_\tau)$ across most of the boundary layer, while (ii) the streamwise velocity is itself small and of $O(u_\tau)$ inside the (exponentially thin) wall layer, and (iii) $u_\tau/U_e = O(1/\ln Re)$. Furthermore, then (iv) the celebrated universal logarithmic velocity distribution

$$u/u_\tau \sim \kappa^{-1} \ln y^+ + C^+ \ , \quad y^+ := y\, u_\tau Re \to \infty \ . \tag{3}$$

is found to hold in the overlap of the outer (small-defect) and inner (viscous wall) layer. Here κ denotes the von Kármán constant; in this connection we note the currently accepted empirical values $\kappa \approx 0.384$, $C^+ \approx 4.1$, which refer to the case of a perfectly smooth surface, see [16] and have been obtained for a zero pressure gradient.

This might be considered to yield a stringent derivation of the logarithmic law of the wall (3), anticipating the existence of an asymptotic state and universality of the wall layer flow as $Re \to \infty$; a view which, however, has been increasingly challenged in more recent publications (e.g. [2–4]). It thus appears that – as expressed by Walker, see [30] – "... although many arguments have been put forward over the years to justify the logarithmic behaviour, non are entirely satisfactory as a proof, ...". As a result, one has to accept that matching (of inner and outer expansions), while ensuring self-consistency, is not sufficient to uniquely determine (3). In the following, from the viewpoint of the time-averaged flow description the logarithmic behaviour (3), therefore, will be taken to represent an experimentally rather than strictly theoretically based result holding in situations where the assumption (b) applies. The description of the boundary layer in the limit $Re \to \infty$ can then

readily be formalised. In passing, we mention that in the classical derivations, see [5,8,10,31], the assumption (b) is not adopted and (3) results from matching, rather than in the present study where it is imposed.

2.2 Leading-Order Approximation

Inside the wall layer where $y^+ = y\,u_\tau Re = O(1)$ the streamwise velocity component u, the Reynolds shear stress $\tau := -\overline{u'v'}$ and the pressure p are expanded in the form

$$u \sim u_\tau(x;Re)\,u^+(y^+) + \cdots\ , \tag{4a}$$

$$\tau \sim u_\tau^2(x;Re)\,t^+(y^+) + \cdots\ , \tag{4b}$$

$$p \sim p_0(x) + \cdots\ , \tag{4c}$$

where u^+ exhibits the limiting behaviour implied by (3):

$$u^+(y^+) \sim \kappa^{-1}\ln y^+ + C^+\ , \quad y^+ \to \infty\ . \tag{5}$$

Assumption (c), quoted in Subsect. 2.1, then uniquely determines the asymptotic expansions of, respectively, u, τ, and p further away from the wall where the Reynolds stress τ is predominant. Let $\delta_{\mathrm{o}}(x;Re)$ characterise the thickness of this outer main layer, i.e. of the overall boundary layer. In turn, one obtains

$$u \sim U_e(x) - u_\tau(x;Re)\,F_1'(x,\eta) + \cdots\ , \tag{6a}$$

$$\tau \sim u_\tau^2(x;Re)\,T_1(x,\eta) + \cdots\ , \tag{6b}$$

$$p \sim p_e(x) + \cdots\ , \tag{6c}$$

where $\eta := y/\delta_{\mathrm{o}}$. Here and in the following primes denote differentiation with respect to η. Furthermore, U_e and p_e stand for the velocity and the pressure, respectively, at the outer edge $\eta = 1$ of the boundary layer (here taken as a sharp line with sufficient asymptotic accuracy) imposed by the external irrotational flow.

Matching of the expansions (4) and (6) by taking into account (5) forces a logarithmic behaviour of F_1',

$$F_1' \sim -\kappa^{-1}\ln\eta + C_0(x)\ , \quad \eta \to 0\ , \tag{7}$$

yields $p_0(x) = p_e(x)$, and is achieved provided $\gamma := u_\tau/U_e$ satisfies the skin-friction relationship

$$\kappa/\gamma \sim \ln(Re\gamma\delta_{\mathrm{o}}U_e) + \kappa(C^+ + C_0) + O(\gamma)\ . \tag{8}$$

From substituting (4) into the x-component (1b) of the Reynolds equations (1) one obtains the well-known result that the total stress inside the wall layer is constant to leading order,

$$\mathrm{d}u^+/\mathrm{d}y^+ + t^+ = 1\ . \tag{9}$$

Moreover, the expansions (6) lead to a linearisation of the convective terms in the outer layer, so that there Bernoulli's law holds to leading order,

$$\mathrm{d}p_e/\mathrm{d}x = -U_e\,\mathrm{d}U_e/\mathrm{d}x\ . \tag{10}$$

The necessary balance with the gradient of the Reynolds shear stress then determines the magnitude of the thickness of the outer layer, i.e. $\delta_\mathrm{o} = O(u_\tau)$. As a consequence, the expansions (6) are supplemented with

$$\delta_\mathrm{o} \sim \gamma\,\Delta_1(x) + \cdots\ , \tag{11}$$

which in turn gives rise to the leading-order outer-layer streamwise momentum equation. After integration with respect to η and and employing the matching condition $T_1(x,0) = 1$, the latter is conveniently written as

$$(E + 2\beta_0)\eta F_1' - EF_1 - \Delta_1 F_{1,e}\,F_{1x} = F_{1,e}(T_1 - 1)\ , \tag{12a}$$

$$F_{1,e} := F_1(x,1)\ , \quad E := 1 - \Delta_1\frac{\mathrm{d}F_{1,e}}{\mathrm{d}x}\ , \quad \beta_0 := -\Delta_1 F_{1,e}\frac{U_{ex}}{U_e}\ . \tag{12b}$$

From here on, the subscript x means differentiation with respect to x. The boundary layer equation (12a) is unclosed, and in order to complete the flow description, turbulence models for t^+ and T_1 have to be adopted. Integration of (12) then provides the velocity distribution in the outer layer and determines the yet unknown function $C_0(x)$ entering (7) and the skin-friction relationship (8), which completes the leading-order analysis.

As a main result, inversion of (8) with the aid of (11) yields

$$\gamma \sim \kappa\sigma[1 - 2\sigma\ln\sigma + O(\sigma)], \quad \sigma := 1/\ln Re\ , \quad \partial\gamma/\partial x = O(\gamma^2)\ . \tag{13}$$

The skin-friction law (13) implies the scaling law (iii), already mentioned in Subsect. 2.1, which is characteristic of classical small-defect flows.

2.3 Second-Order Outer Problem

Similar to the description of the leading-order boundary layer behaviour, the investigation of higher-order effects is started by considering the wall layer first. Substitution of (4a), (4b), (8) into (1b) yields upon integration (cf. [30]),

$$\frac{1}{Re}\frac{\partial u}{\partial y} + \tau \sim \gamma^2 U_e^2 - \frac{U_e U_{ex}}{\gamma Re}\,y^+ + \frac{\gamma U_e U_{ex}}{Re}\int_0^{y^+} {u^+}^2\,\mathrm{d}y^+ + \cdots\ . \tag{14}$$

Here the second and third terms on the right-hand side account, respectively, for the effects of the (imposed) pressure gradient, c.f. (10), and convective terms, which have been neglected so far. By using (5) and (12), the asymptotic behaviour of τ as $y^+ \to \infty$ can easily be obtained (e.g. [30]). Rewritten in terms of the outer-layer variable η, it is found to be described by

$$\frac{\tau}{U_e^2} \sim \gamma^2\left[1 + 2\frac{\Delta_0 U_{ex}}{\kappa U_e}\eta\ln\eta + \cdots\right] + \gamma^3\left[\frac{\Delta_0 U_{ex}}{\kappa^2 U_e}\eta(\ln\eta)^2 + \cdots\right] + \cdots\ , \tag{15}$$

as $\eta \to 0$, which immediately suggests the appropriate generalisation of the small-defect expansions (6a), (6b), (11):

$$u/U_e \sim 1 - \gamma F_1' - \gamma^2 F_2' + \cdots \,, \tag{16a}$$

$$\tau/U_e^2 \sim \gamma^2 T_1 + \gamma^3 T_2 + \cdots \,, \tag{16b}$$

$$\delta_{\mathrm{o}} \sim \gamma\, \Delta_1(x) + \gamma^2 \Delta_2(x) + \cdots \,. \tag{16c}$$

Here matching with the wall layer is achieved if

$$F_1' \sim -\kappa^{-1} \ln \eta + C_0(x) \,, \quad F_2' \sim C_1(x) \,, \tag{17a}$$

$$T_1 \sim 1 + 2\frac{\Delta_0 U_{ex}}{\kappa U_e}\eta \ln \eta \,, \quad T_2 \sim \frac{\Delta_0 U_{ex}}{\kappa^2 U_e}\eta (\ln \eta)^2 \,, \tag{17b}$$

as $\eta \to 0$, provided that the skin-friction relationship (8) is modified to explicitly include an additional term of $O(\gamma)$,

$$\kappa/\gamma \sim \ln(Re\gamma\delta_{\mathrm{o}} U_e) + \kappa(C^+ + C_0 + \gamma C_1) + \cdots \,. \tag{18}$$

Similar to $C_0(x)$, the function $C_1(x)$ depends on the specific turbulence model adopted, as well as the upstream history of the boundary layer.

2.4 Can Classical Small-Defect Theory Describe Boundary Layer Separation?

An estimate of the thickness δ_{w} of the viscous wall layer is readily obtained from the definition of y^+, see (3), and the (inverted) skin-friction relationship (13): $\delta_{\mathrm{w}} = O[\gamma^{-1} \exp(-\kappa/\gamma)]$. In the limit $Re \to \infty$, therefore, the low-momentum region close to the wall is exponentially thin as compared to the outer layer, where Reynolds stresses cause a small $O(\gamma)$-reduction of the fluid velocity with respect to the mainstream velocity $U_e(x)$. This theoretical picture of a fully attached turbulent small-defect boundary layer has been confirmed by numerous comparisons with experimental data for flows of this type (e.g. [1,14,30]). However, it also indicates that attempts based on this picture to describe the phenomenon of boundary layer separation, frequently encountered in engineering applications, will face serious difficulties. Since the momentum flux in the outer layer, which comprises most of the boundary layer, differs only slightly from that in the external flow region, an $O(1)$-pressure rise almost large enough to cause flow reversal even there appears to be required to generate negative wall shear, which hardly can be considered as flow separation. This crude estimate is confirmed by a more detailed analysis dealing with the response of a turbulent small-defect boundary layer to a surface-mounted obstacle, carried out, among others, in [28]. Moreover, to date no self-consistent theory of flow separation compatible with the classical concept of a turbulent small-defect boundary layer has been formulated.

The above considerations strikingly contrast the case of laminar boundary layer separation, where the velocity defect is of $O(1)$ across the whole boundary layer and the associated pressure increase tends to zero as $Re \to \infty$. It,

however, also indicates that a turbulent boundary layer may become more prone to separation by increasing the velocity defect. That this is indeed a realistic scenario can be inferred by seeking self-preserving solutions of (12), i.e. by investigating equilibrium boundary layers. Such solutions, where the functions F_1, T_1, characterising the velocity deficit and the Reynolds shear stress in the outer layer, respectively, solely depend on η, exist if the parameter β_0 in the outer-layer momentum equation (12a) is constant, i.e. independent of x. Equation (12a) then assumes the form

$$(1+2\beta_0)\eta F_1' - F_1 = F_{1,e}(T_1-1)\ , \tag{19}$$

where

$$U_e \propto (x-x_\mathrm{v})^m\ , \quad m=-\beta_0/(1+3\beta_0)\ , \quad \Delta_1 F_{1,e} = (1+3\beta_0)(x-x_\mathrm{v})\ . \tag{20}$$

Herein $x=x_\mathrm{v}$ denotes the virtual origin of the boundary layer flow. In the present context flows associated with large values of β_0 are of most interest. By introducing suitably (re)scaled quantities in the form $F_1=\beta_0^{1/2}\hat{F}(\hat{\eta})$, $T_1=\beta_0\hat{T}(\hat{\eta})$, $\eta=\beta_0^{1/2}\hat{\eta}$, the momentum equation (19) reduces to

$$2\hat{\eta}\hat{F}' = \hat{F}_e\hat{T}\ , \quad \hat{F}_e := \hat{F}(1) \tag{21}$$

in the limit $\beta_0\to\infty$. Solutions of (21) describing turbulent boundary layers having a velocity deficit measured by $u_\mathrm{ref}:=\beta_0^{1/2}u_\tau \gg u_\tau$ have been obtained first in [11]. Unfortunately, however, it was not realised that this increase of the velocity defect no longer allows for a direct match of the flow quantities in the outer and inner layer, which has significant consequences, to be elucidated below.

We note that in general $\beta_0(x)$ can be regarded as the leading-order contribution to the so-called Rotta–Clauser pressure-gradient parameter (e.g. [24]),

$$\beta := -U_eU_{ex}\delta^*/u_\tau^2\ , \quad \delta^* := \delta_\mathrm{o}\int_0^\infty (1-u/U_e)\,\mathrm{d}\eta\ . \tag{22}$$

As already mentioned in [11], this quantity allows for the appealing physical interpretation that u_ref is independent of the wall shear stress u_τ^2 for $\beta_0\gg 1$.

3 Moderately Large Velocity Defect

Following the considerations summarised in the preceding section, we now seek solutions of (1) describing a relative velocity defect of $O(\varepsilon)$, where the newly introduced perturbation parameter ε is large compared to γ but still small compared to one: $\gamma\ll\varepsilon\ll 1$. From assumption (a), see Subsect. 2.1, we then have $-\overline{u'v'}\sim\varepsilon^2$, and the linearised x-momentum equation immediately yields the estimate $\delta_\mathrm{o}=\varepsilon\Delta$, where $\Delta=O(1)$, for the boundary layer

thickness. However, since $-\overline{u'v'} \sim \varepsilon^2$ with $\varepsilon \gg u_\tau^2$, the solution describing the flow behaviour in the outer velocity defect region no longer matches with the solution for the universal wall layer as in the classical case. As a consequence, the leading-order approximation to the Reynolds shear stress must vanish in the limit $\eta = y/\delta_\mathrm{o} \to 0$. This indicates that the flow having a velocity defect of $O(\varepsilon)$ in the outer main part of the boundary layer exhibits a wake-type behaviour, leading to a finite wall slip velocity at its base and, therefore, forces the emergence of a sublayer, termed intermediate layer, where the magnitude of $-\overline{u'v'}$ reduces to $O(u_\tau^2)$, being compatible with the wall layer scaling.

3.1 Intermediate Layer

Here the streamwise velocity component u is expanded about its value at the base $\eta = 0$ of the outer defect region: $u/U_e \sim 1 - \varepsilon W - \gamma U_\mathrm{i} + \cdots$, so that the quantities W, U_i, assumed to be of $O(1)$, account, respectively, for the wall slip velocity, given by $u = U_e(1 - \varepsilon W)$ with $W > 0$, and the dominant contribution to u that varies with distance y from the wall. Integration of the x-momentum balance then shows that the Reynolds shear stress increases linearly with distance y for $y/\delta_\mathrm{o} \ll 1$:

$$\tau \sim \tau_w - \varepsilon (U_e^2 W)_x y \;, \quad y/\delta_\mathrm{i} = O(1) \;. \tag{23}$$

Herein δ_i denotes the thickness of the intermediate layer and τ assumes its near-wall value τ_w as $y/\delta_\mathrm{i} \to 0$. Matching with the wall layer then requires that $\tau_w \sim u_\tau^2$, which, by taking into account (22), yields the estimate $\delta_\mathrm{i}/\delta_\mathrm{o} = O(\beta^{-1})$. Also, since $\tau_w \sim u_\tau^2$, we infer that $\delta_\mathrm{i} = O(u_\tau^2/\varepsilon)$ and, in turn, recover the relationship $\varepsilon \sim u_\tau \beta^{1/2}$, already suggested by the final considerations of Subsect. 2.4. Formal expansions of u and $-\overline{u'v'}$ in the intermediate layer, therefore, are written as

$$u/U_e \sim 1 - \varepsilon W(x;\varepsilon,\gamma) - \gamma U_\mathrm{i}(x,\zeta) \;, \tag{24a}$$

$$-\overline{u'v'}/(\gamma U_e)^2 \sim T_\mathrm{i}(x,\zeta;\varepsilon,\gamma) \sim 1 + \lambda\zeta \;, \tag{24b}$$

where $\zeta := y/\delta_\mathrm{i} = y\varepsilon/(\Delta\gamma^2)$ and $\lambda := -\Delta(U_e^2 W)_x/U_e^2$.

To close the problem for U_i, we adopt the common mixing length concept,

$$-\overline{u'v'} := \ell^2 \frac{\partial u}{\partial y}\left|\frac{\partial u}{\partial y}\right| \;, \tag{25}$$

by assuming that the mixing length ℓ behaves as $\ell \sim \kappa y$ for $y = O(\delta_\mathrm{i})$, which is the simplest form allowing for a match with the adjacent layers. Integration of (24b), supplemented with (25), then yields

$$\kappa U_\mathrm{i} = -\ln\zeta + 2\ln\left[(1+\lambda\zeta)^{1/2} + 1\right] - 2(1+\lambda\zeta)^{1/2} \;, \tag{26}$$

from which the limiting forms

$$\kappa U_{\rm i} \sim -2(\lambda\zeta)^{1/2} + (\lambda\zeta)^{-1/2} + O(\zeta^{-3/2}) \;, \quad \zeta \to \infty \;, \tag{27a}$$

$$\kappa U_{\rm i} \sim -\ln(\lambda\zeta/4) - 2 - \lambda\zeta/2 + O(\zeta^2) \;, \qquad \zeta \to 0 \;, \tag{27b}$$

can readily be inferred. The behaviour (27a) holding at the base of the outer defect layer is recognised as the square-root law deduced first by Townsend in his study [29] of turbulent boundary layers exhibiting vanishingly small wall shear stress; the outermost layer so to speak "anticipates" the approach to separation as the velocity defect increases to a level larger than u_τ. We remark that Townsend in [29] identified the intermediate region as the so-called "equilibrium layer", where convective terms in (1b) are (erroneously within the framework of asymptotic high-Reynolds-number theory) considered to be negligibly small. Equation (27b) provides the logarithmic variation of $U_{\rm i}$ as $\zeta \to 0$, required by the match with the wall layer, which gives rise to the generalised skin-friction relationship

$$\frac{\kappa}{\gamma} \sim \ln\left(\frac{Re\gamma^2 U_e^3}{\beta_0^{1/2}}\right) + \beta_0\kappa W + O(\gamma\beta_0) \sim (1+\varepsilon W)\ln Re \;. \tag{28}$$

Note that (28) reduces to (8) when $\beta_0 = O(1)$.

Having demonstrated that classical theory of turbulent boundary layers in the limit of large Reynolds number can – in a self-consistent manner – be extended to situations where the velocity defect is asymptotically large as compared to u_τ but still $o(1)$, we now consider the flow behaviour in the outer wake-type region in more detail.

3.2 Outer Defect Region

Following the arguments put forward at the beginning of Sect. 3, we write, by making use of the stream function ψ, the flow quantities in the outer layer in the form

$$p \sim p_e(x) + \varepsilon^2 P(x,\eta;\varepsilon,\gamma) \;, \tag{29a}$$

$$\psi/U_e \sim y - \varepsilon\delta_o F(x,\eta;\varepsilon,\gamma) \;, \tag{29b}$$

$$-\left[\overline{u'^2}, \overline{v'^2}, \overline{u'v'}\right] \sim U_e^2\varepsilon^2[R,S,T](x,\eta;\varepsilon,\gamma) \;. \tag{29c}$$

As before, here $\eta = y/\delta_{\rm o}$ and we accordingly expand

$$Q \sim Q_1 + \varepsilon\, Q_2 + \cdots \;, \quad Q := F,P,R,S,T,W \;, \tag{30a}$$

$$\delta \sim \varepsilon\Delta_1 + \varepsilon^2\Delta_2 + \cdots \;, \tag{30b}$$

$$\beta/\beta_{\rm v} \sim B_0(x) + \varepsilon B_1(x) + \cdots \;, \quad \beta_{\rm v} \to \infty \;, \tag{30c}$$

where we require (without any loss of generality) that $\beta_{\rm v}$ equals β_0 at $x = x_{\rm v}$, so that $\beta_0 = \beta_{\rm v} B_0$ and $B_0(x_{\rm v}) = 1$, $B_i(x_{\rm v}) = 0$, $i = 1, 2, \ldots$. In analogy to (12), the first-order problem then reads

$$\frac{1}{U_e}\frac{\mathrm{d}(U_e\Delta_1)}{\mathrm{d}x}\eta F_1' - \frac{1}{U_e^3}\frac{\partial(U_e^3\Delta_1 F_1)}{\partial x} = T_1 \ , \tag{31a}$$

$$F_1(x,0) = F_1'(x,1) = F_1''(x,1) = T_1(x,1) = 0 \ , \tag{31b}$$

$$\eta \to 0: \quad T \sim (\kappa\eta F_1'')^2 \ , \quad F_1' \sim W_1(x) - (2/\kappa)(\lambda\eta)^{1/2} \ . \tag{31c}$$

In the following we concentrate on solutions which are self-similar up to second order, i.e. $\partial F_1/\partial x \equiv \partial T_1/\partial x \equiv 0$ and $\partial F_2/\partial x \equiv \partial T_2/\partial x \equiv 0$. By again adopting the notations $F_1 = \hat{F}(\eta)$, $T_1 = \hat{T}(\eta)$, and setting $\Delta_1 = \hat{\Delta}(x)$, $U_e = \hat{U}(x)$, we recover the requirements (20), (21) for self-similarity at first order resulting from classical small-defect theory in the limit of large values of β_v, in agreement with (30b) and the definition of β provided by (22):

$$B_0 \equiv 1 \ , \quad \hat{\Delta}\hat{F}_e = 3(x - x_\mathrm{v}) \ , \quad \hat{U} = (C/3)^{1/3}(x - x_\mathrm{v})^{-1/3} \ , \tag{32}$$

with a constant C, and

$$2\eta\hat{F}' = \hat{F}_e\hat{T} \ , \quad \hat{F}(0) = \hat{T}(0) = \hat{F}'(1) = \hat{F}''(1) = \hat{T}(1) = 0 \ . \tag{33}$$

If, as in the discussion of the flow behaviour in the intermediate layer, a mixing length model $\hat{T} = [\ell(\eta)\hat{F}''(\eta)]^2$ in accordance with (25) is chosen to close the problem, integration of (33) yields the analytical expressions

$$\hat{F}'(\eta) = \frac{1}{2\hat{F}_e}\left[\int_\eta^1 \frac{z^{1/2}}{\ell(z)}\,\mathrm{d}z\right]^2 \ , \quad \hat{F}_e = \left\{\frac{1}{2}\int_0^1 \left[\int_\eta^1 \frac{z^{1/2}}{\ell(z)}\,\mathrm{d}z\right]^2 \mathrm{d}\eta\right\}^{1/2} \ . \tag{34}$$

Equations (34) have been evaluated numerically by using a slightly generalised version of the mixing length closure originally suggested in [13],

$$\ell = c_\ell I(\eta)^{1/2}\tanh(\kappa\eta/c_\ell) \ , \quad I = 1/(1 + 5.5\eta^6) \ , \quad c_\ell = 0.085 \ . \tag{35}$$

Herein $I(\eta)$ represents the well-known Klebanoff's intermittency factor proposed in [9]. One then obtains $W_1 = \hat{F}'(0) \doteq 13.868$, $\hat{F}_e \doteq 5.682$, and $\mathrm{d}\hat{\Delta}/\mathrm{d}x \doteq 0.528$, cf. (32). As seen in Fig. 1a, both $\hat{F}'$ and $\hat{T}$ vanish quadratically as $\eta \to 1$ as a result of the boundary conditions $\hat{T}(1) = \hat{T}'(1) = 0$, cf. (33). Also, note that $\hat{F}'$ exhibits the square-root behaviour required from the match with the intermediate layer as $\eta \to 0$.

Turning now to the second-order problem, we consider the most general case that the wall shear enters the description of the flow in the outer layer at this level of approximation (principle of least degeneracy). Therefore, we require $\varepsilon^3 T_2(0) \sim \gamma^2$, which finally determines the yet unknown magnitude of ε relative to γ, namely that $\varepsilon \sim \gamma^{2/3}$. Since, as pointed out before, $\varepsilon \sim \gamma\beta_0^{1/2}$, this implies that $\varepsilon\beta_0 = \Gamma = O(1)$. Inspection of the resulting second-order problem indicates that self similar solutions exist only if the external velocity distribution (32) predicted by classical theory is slightly modified in the form

$$\hat{U}(x) = (C/3)^{1/3}(x - x_\mathrm{v})^{-1/3+\mu}, \quad \mu \sim \gamma^{2/3}\mu_1 + \cdots \ , \tag{36}$$

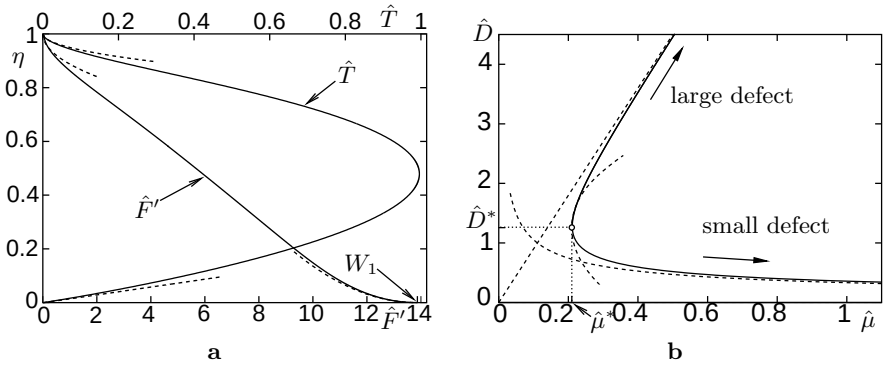

Fig. 1. Quasi-equilibrium flows: (**a**) $\hat{F}'(\eta)$, $\hat{T}(\eta)$, *dashed*: asymptotes found from (31b), (31c); (**b**) canonical representation (37), *dashed*: asymptotes (see last paragraph of Sect. 3) and parabola approximating the curve in the apex to leading order

where the $O(1)$-parameter μ_1 satisfies a solvability condition that represents the integral momentum balance obtained from integrating the second-order x-momentum equation from $\eta = 0$ to $\eta = 1$. It can be cast into the canonical form

$$9\hat{D}^2\hat{\mu} = 1 + \hat{D}^3 \; . \tag{37}$$

Herein $\hat{D} = r^{1/3}\Gamma^{1/3}$, $\hat{\mu} = r^{-2/3}\mu_1$, and

$$r = \hat{F}_e^{-1} \int_0^1 (\hat{F}'^2 - \hat{R} + \hat{S}) \, \mathrm{d}\eta \; . \tag{38}$$

A graph of the relationship (37) which represents the key result of the analysis dealing with quasi-equilibrium boundary layers having a moderately large velocity defect is shown in Fig. 1b. Most interesting, it is found that solutions describing flows of this type exist for $\hat{\mu} \geq \hat{\mu}^* = 2^{1/3}/6$ only and form two branches, associated with non-uniqueness of the quantity $\hat{D}$, which serves as a measure of velocity defect, for a specific value of the pressure gradient. Along the lower branch, $\hat{D} \leq \hat{D}^* = 2^{1/3}$ and decreases with increasing values of $\hat{\mu}$, so that classical small-defect theory is recovered in the limit $\hat{\mu} \to \infty$, where $\hat{D} \sim (9\hat{\mu})^{-1/2}$. In contrast, this limit leads to an unbounded growth of values $\hat{D} \geq \hat{D}^*$ associated with the upper branch: $\hat{D} \sim 9\hat{\mu}$ as $\hat{\mu} \to \infty$. This immediately raises the question if it is possible to formulate a general necessarily nonlinear theory which describes turbulent boundary layers having a finite velocity defect in the limit of infinite Reynolds number. We also note that the early experimental observations made by Clauser, see [6], seem to strongly point to this type of non-uniqueness.

4 Large Velocity Deficit

As in the cases of small and moderately small velocity defect we require the boundary layer to be slender. However, in contrast to the considerations of Sects. 2 and 3, the validity of this requirement can no longer be inferred from assumption (a) and the balance between convective and Reynolds stress gradient terms in the outer predominately inviscid region of the boundary layer which now yields $\partial\tau/\partial y = O(1)$, rather than $\partial\tau/\partial y \ll 1$ as earlier. A hint how this difficulty can be overcome is provided by the observation that the transition from a small to a moderately large velocity defect is accompanied with the emergence of a wake-type flow in this outer layer. One expects that this effect will become more pronounced as the velocity defect increases further, suggesting in turn that the outer part of the boundary layer, having a velocity defect of $O(1)$, essentially behaves as a turbulent free shear layer. An attractive strategy then is to combine the asymptotic treatment of such flows (e.g. [25]) in which the experimentally observed slenderness is enforced through the introduction of a Reynolds-number-independent parameter $\alpha \ll 1$ with the asymptotic theory of turbulent wall bounded flows.

4.1 Outer Wake Region

Let the parameter $\alpha \ll 1$ measure the lateral extent of the outer wake region, so that $\bar{y} := y/\alpha = O(1)$. Appropriate expansions of the various field quantities then are

$$p \sim p_e(x) + O(\alpha) \,, \tag{39a}$$

$$q \sim \alpha\, q_0(x,\bar{y}) + o(\alpha) \,, \tag{39b}$$

where q stands for Δ, ψ, $\tau := -\overline{u'v'}$, $\sigma_{(x)} := -\overline{u'^2}$, $\sigma_{(y)} := -\overline{v'^2}$. From substitution into (1b–1c) the leading order outer wake problem is found to be

$$\frac{\partial\psi_0}{\partial\bar{y}}\frac{\partial^2\psi_0}{\partial\bar{y}\partial x} - \frac{\partial\psi_0}{\partial x}\frac{\partial^2\psi_0}{\partial\bar{y}^2} = -U_e U_{ex} + \frac{\partial\tau_0}{\partial\bar{y}} \,, \tag{40a}$$

$$\bar{y} = 0: \quad \psi_0 = \tau_0 = 0 \,, \tag{40b}$$

$$\bar{y} = \Delta_0(x): \quad \partial\psi_0/\partial\bar{y} = U_e \,, \quad \tau_0 = 0 \,. \tag{40c}$$

As in the case of a moderately large velocity defect, we expect a finite wall slip $U_s(x) := \partial\psi_0/\partial\bar{y}$ at the base $\bar{y} = 0$ of this outer layer, which yields the limiting behaviour

$$\partial\psi_0/\partial\bar{y} \sim U_s(x) + O(\bar{y}^{3/2}) \,, \quad \tau_0 \sim \Lambda_0\bar{y} + O(\bar{y}^{3/2}) \,, \tag{41}$$

with $\Lambda_0 := U_s U_{sx} - U_e U_{ex} > 0$.

It is easily verified that the various layers introduced so far in the description of turbulent boundary layers share the property that their lateral extent is of the order of the mixing length ℓ characteristic for the respective

layer. In contrast, the scalings given by (39) imply that ℓ is much smaller than the thickness of the outer wake region: $\ell \sim \alpha^{3/2} \ll \alpha$. This is a characteristic feature of free shear layers, of course, but also indicates that the outer wake region "starts to feel" the presence of the confining wall at distances $y \sim \alpha^{3/2}$, which in turn causes the emergence of an inner wake region.

4.2 Inner Wake Region

By introducing the stretched wall distance $Y = y/\alpha^{3/2} = O(1)$, inspection of (41) suggests the expansions

$$\psi \sim \alpha^{3/2} U_s(x) + \alpha^{9/4} \bar{\psi}(x, Y) + \cdots , \tag{42a}$$

$$\tau \sim \alpha^{3/2} \bar{T}(x, Y) + \cdots , \quad \ell \sim \alpha^{3/2} \bar{L}(x, Y) + \cdots , \tag{42b}$$

which leads to

$$\bar{T} = \Lambda_0 Y . \tag{43}$$

Furthermore, $\bar{T}$ and $\bar{\psi}$ are subject to the boundary conditions

$$T(x, 0) = \bar{\psi}(x, 0) = 0 , \tag{44a}$$

$$\bar{\psi}_Y \sim \frac{2}{3} \frac{\Lambda_0^{1/2}}{\bar{L}_0} Y^{3/2} , \quad Y \to \infty , \quad \bar{L}_0 = \lim_{Y \to \infty} \bar{L} . \tag{44b}$$

The solution of the inner wake problem posed by (43), (44) can be obtained in closed form. It exhibits the expected square-root behaviour of $\bar{\psi}_Y$,

$$\bar{\psi}_Y \sim \bar{U}_s(x) + 2 \frac{(\Lambda_0 Y)^{1/2}}{\chi(x)} , \quad \bar{L} \sim \chi(x) \bar{Y} , \quad Y \to 0 . \tag{45}$$

Here $\bar{U}_s(x)$ denotes the correction of the slip velocity $U_s(x)$ caused by the inner wake region,

$$u_s \sim U_s(x) + \alpha^{3/4} \bar{U}_s(x) + \cdots , \tag{46a}$$

$$\bar{U}_s(x) = - \int_0^\infty \left(\frac{1}{\bar{L}} - \frac{1}{\bar{L}_0} \right) (\Lambda_0 Y)^{1/2} \, \mathrm{d}Y . \tag{46b}$$

At this point it is important to recall the basic assumption made at the beginning of this section, namely, that the slenderness parameter α is independent of Re, or more generally, asymptotes to a small but finite value as $Re \to \infty$. As a consequence, the outer and inner wake regions provide a complete description of the boundary layer flow in the formal limit $Re^{-1} = 0$. If, however, $0 < 1/Re \ll 1$ an additional sublayer forms at the base of the inner wake region. This sublayer plays a similar role as the intermediate layer discussed in Subsect. 3.1: there the magnitude of the Reynolds shear stress, still varying linearly with distance from the wall, is reduced to $O(u_\tau^2)$, which is necessary to provide the square-root behaviour expressed in (45) and, finally, to allow for the match with the universal wall layer, see [19].

4.3 Numerical Solution of the Leading-Order Outer-Wake Problem

As earlier, a slightly modified version of the mixing length model proposed in [13] will be adopted to close the outer wake problem posed by (40). Numerical calculations were carried out for a family of retarded external flows controlled by two parameters m_s, k, with $m_s < 0$, $0 \le k < 1$:

$$U_e(x; m_s, k) = (1+x)^{m(x;m_s,k)} \,, \tag{47a}$$

$$\frac{m}{m_s} = 1 + \frac{k}{1-k}\,\Theta(2-x)\big[1-(1-x)^2\big]^3 \,. \tag{47b}$$

Herein Θ denotes the Heaviside step function. Self-similar solutions of the form $\psi_0 = \Delta_0 F(\xi)$, $\xi := Y/\Delta_0$, $\Delta_0 = b(1+x)$, where $b = \text{const}$ and the position $x = -1$ defines the virtual origin of the flow, exist for $k = 0$ if $m_s > -1/3$ and are used to provide initial conditions at $x = 0$ for the downstream integration of (40) with U_e given by (47). As a specific example, we consider the case $F'(0) = 0.95$ of a relatively small velocity defect, imposed at $x = 0$, for which the requirement of self-similarity for $-1 < x < 0$ yields $b \doteq 0.3656$ and $m_s \doteq -0.3292$. The key results which are representative for the responding boundary layer and, most important, indicate that the present theory is capable of describing the approach to separation are displayed in Fig. 2. If k is sufficiently small, the distribution of the wall slip velocity U_s is smooth and $U_s > 0$ throughout. However, when k reaches a critical value $k_M \doteq 0.84258$, the slip velocity U_s is found to vanish at a single location $x = x_M$, but is positive elsewhere. A further increase of k provokes a breakdown of the calculations, accompanied with the formation of a weak singularity slightly upstream of x_M at $x = x_G$. A similar behaviour is observed for the boundary layer thickness Δ_0, which is smooth in the subcritical case $k < k_M$, exhibits a rather sharp peak $\Delta_{0,M}$ for $k = k_M$ at $x = x_M$, and approaches a finite limit $\Delta_{0,G}$ in an apparently singular manner in the supercritical case $k > k_M$.

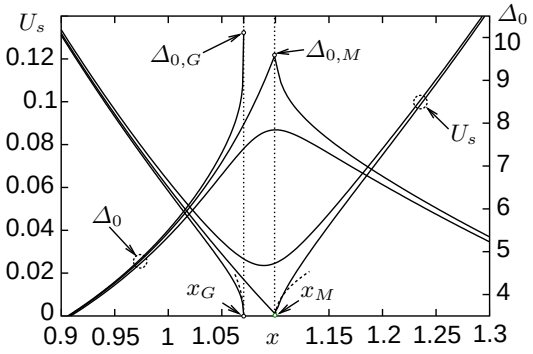

Fig. 2. Solutions of (40) for $|x - x_M| \ll 1$, $|k - k_M| \ll 1$, *dashed*: asymptotes expressed by (48b), (49)

Following the qualitatively similar behaviour of the wall shear stress that replaces U_s in the case of laminar boundary layers, see [17, 18, 27], the critical solution with $k = k_M$ is termed a marginally separating boundary layer solution. However, in vivid contrast to its laminar counterpart, is is clearly seen to be locally asymmetric with respect to $x = x_M$ where it is singular. This numerical finding is supported by a local analysis of the flow behaviour near $x = x_M$, carried out in [20]: it indicates that U_s decreases linearly with x upstream of $x = x_M$ but exhibits a square-root singularity as $x - x_M \to 0_+$,

$$U_s/P_{00}^{1/2} \sim -B(x - x_M) \,, \qquad x - x_M \to 0_- \,, \tag{48a}$$

$$U_s/P_{00}^{1/2} \sim U_+(x - x_M)^{1/2} \,, \quad x - x_M \to 0_+ \,, \tag{48b}$$

where $P_{00} = (\mathrm{d}p_e/\mathrm{d}x)(x_M)$. It is found that $U_+ \doteq 1.1835$, whereas the constant B remains arbitrary in the local investigation and has to be determined by comparison with the numerical results for $x \leq x_M$.

This local analysis also shows that a square-root singularity forms at a position $x = x_G < x_M$ for $k > k_M$,

$$U_s/P_{00}^{1/2} \sim U_-(x_G - x)^{1/2} \,, \quad x - x_G \to 0_- \,, \tag{49}$$

with some U_- to be determined numerically, and that the solution cannot be extended further downstream. This behaviour, which has been described first in [12], is reminiscent of the Goldstein singularity well-known from the theory of laminar boundary layers and, therefore, will be termed the turbulent Goldstein singularity. As shown in the next section, the bifurcating behaviour of the solutions for $k - k_M \to 0$ is associated with the occurrence of marginally separating flow.

4.4 Marginal Separation

According to the original boundary layer concept, pressure disturbances caused by the displacement of the external inviscid flow due to the momentum deficit, which is associated with the reduced velocities close to the wall, represent a higher order effect. Accordingly, higher-order corrections to the leading-oder approximation of the flow quantities inside and outside the boundary layer can be calculated in subsequent steps. However, as found first for laminar flows, this so-called hierarchical structure of the perturbation scheme breaks down in regions where the displacement thickness changes so rapidly that the resulting pressure response is large enough to affect the lowest-order boundary layer approximation (e.g. [26]). A similar situation is encountered for the type of turbulent flows discussed in the preceding section. Indeed, the slope discontinuity of Δ_0 and, in turn, of the displacement thickness forces a singularity in the response pressure, indicating a breakdown of the hierarchical approach to boundary layer theory. As for laminar flows, see [17, 18, 27], this deficiency can be overcome by adopting a local interaction strategy, so

that the induced pressure disturbances enter the description of the flow in leading rather than higher order.

Again, similar to laminar flows, three layers (decks) characterising regions of different flow behaviour have to be distinguished inside the local interaction region, see Fig. 3. Effects of Reynolds stresses are found to be confined to the lower deck region (LD), having a streamwise and lateral extent of $O(\alpha^{3/5})$ and $O(\alpha^{6/5})$, respectively. Here the flow is governed by equations of the form (40). The majority of the boundary layer, i.e. the main deck (MD), behaves passively in the sense that it transfers displacement effects caused by the lower deck region unchanged to the external flow region taking part in the interaction process, the so-called upper deck (UD), and transfers the resulting pressure response unchanged to the lower deck. Solutions to the leading-order main and upper deck problems can be obtained in closed form which finally leads to the fundamental lower deck problem. By using suitably stretched variables, it can be written in terms of a stream function $\hat{\psi}(\hat{X},\hat{Y})$ as (see [20])

$$\frac{\partial\hat{\psi}}{\partial\hat{Y}}\frac{\partial^2\hat{\psi}}{\partial\hat{Y}\partial\hat{X}}-\frac{\partial\hat{\psi}}{\partial\hat{X}}\frac{\partial^2\hat{\psi}}{\partial\hat{Y}^2}=-1-\Lambda(\Gamma)\,\hat{P}'(\hat{X})+\frac{\partial\hat{T}}{\partial\hat{Y}}\,, \tag{50a}$$

$$\hat{T}=\frac{\partial^2\hat{\psi}}{\partial\hat{Y}^2}\left|\frac{\partial^2\hat{\psi}}{\partial\hat{Y}^2}\right|\,, \tag{50b}$$

$$\hat{P}(\hat{X})=\frac{1}{\pi}\,\text{⨍}\!\!\!\!\!\!-\!\!\int_{-\infty}^{\infty}\frac{\hat{A}'(\hat{S})}{\hat{X}-\hat{S}}\,\mathrm{d}\hat{S} \tag{50c}$$

$$\hat{Y}=0:\quad \hat{\psi}=\hat{T}=0\,, \tag{50d}$$

$$\hat{Y}\to\infty:\quad \hat{T}-\hat{Y}\to\hat{A}(\hat{X})\,, \tag{50e}$$

$$\hat{X}\to-\infty:\quad \hat{\psi}\to(4/15)\hat{Y}^{5/2}+\Gamma\hat{Y}\,,\quad 0\le\Gamma\le1\,, \tag{50f}$$

$$\hat{X}\to\infty:\quad \hat{\psi}\to\hat{X}^{5/6}F_+(\hat{\eta})\,,\quad \hat{\eta}:=\hat{Y}/\hat{X}^{1/3}\,. \tag{50g}$$

The first and second term on the right-hand side of (50a) account for the imposed and induced pressure, respectively. The latter is given by the Hilbert integral (50c), where $\hat{A}$ characterises the displacement effect exerted by the lower deck region. The far-field condition (50e) expresses the passive character of the main deck mentioned before, whereas the conditions (50f), (50g) follow from the match with regions LD_-, LD_+ immediately upstream and downstream of the local interaction zone. The analysis of region LD_+ determines the function $F_+(\hat{\eta})$. Finally, the parameter Γ measures the intensity of the interaction process as the monotonically increasing but otherwise arbitrary function $\Lambda(\Gamma)$ expresses the magnitude of the induced pressure gradient.

As a representative example of flows encountering separation, the distributions of $\hat{A}$, $\hat{P}$, and the wall slip $\hat{U}_s:=(\partial\hat{\psi}/\partial\hat{Y})(\hat{X},\hat{Y}=0)$, obtained by numerical solution of the triple-deck problem (50) for $\Gamma=0.019$, $\Lambda=3$, are depicted in Fig. 4a. Here the dot-and-dash lines indicate the upstream and downstream asymptotes, obtained from the analysis of the flow behaviour in the pre- and post-interaction regions (subscripts "−" and "+" in Fig. 3), while

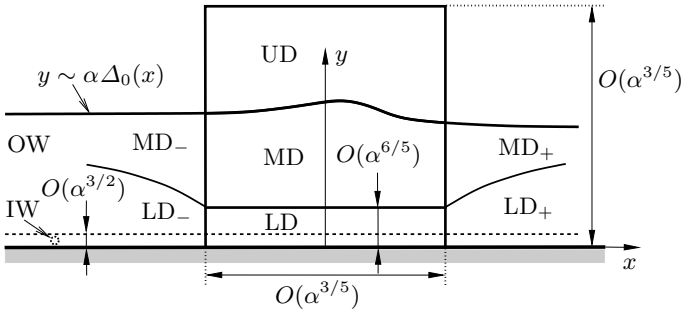

Fig. 3. Triple-deck structure, for captions see text, subscripts "−" and "+" refer to the continuation of flow regions up- and downstream of the local interaction zone, *dashed* line indicates inner wake

$\hat{X}_D$ and $\hat{X}_R$ denote the positions of, respectively, detachment and reattachment. It is interesting to note that the passage of $\hat{U}_s$ into the reverse-flow region where $\hat{U}_s < 0$ causes the interaction pressure $\hat{P}$ to drop initially before it rises sharply, overshoots and finally tends to zero in the limit $\hat{X} \to \infty$. This is in striking contrast to laminar flows, where flow separation always is triggered by an initial pressure rise, and reflects the fact that – in the case of turbulent flows considered here – the streamwise velocity component at the base $\hat{Y} = 0$ of the lower deck region is allowed to take on finite values, whereas the no-slip condition is enforced in its laminar counterpart.

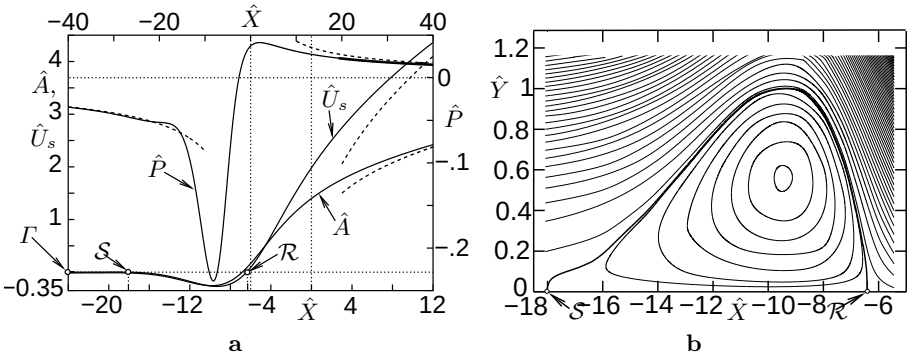

Fig. 4. Specific solution of (50), separation in $\mathcal{S}$, reattachment in $\mathcal{R}$: (**a**) key quantities, *dashed*: asymptotes found analytically; (**b**) streamlines

Streamlines inside the lower-deck region are displayed in Fig. 4b which clearly shows the formation of a recirculating eddy. Also, we draw attention to the increasing density of streamlines further away from the wall and downstream of reattachment, associated with the strong acceleration of the fluid there as evident from the rapid increase of $\hat{U}_s$.

The interaction process outlined so far describes the behaviour or marginally separated turbulent flows in the limit $1/Re = 0$. As in the case of conventional, i.e. hierarchical, boundary layers having a velocity of defect of $O(1)$, additional sublayers form closer to the wall if $1/Re \ll 1$ but finite. Their analysis, outlined in [19], provides the skin-friction relationship in generalised form to include the effects of vanishing and negative wall shear – treated first in a systematic way in [24] – but also shows that these layers behave passively insofar as the lower deck problem (50) remains intact.

5 Conclusions and Outlook

In this study an attempt has been made to derive the classical two-layer structure of a turbulent small-defect boundary layer from a minimum of assumptions. As in [30], but in contrast to earlier investigations (e.g. [10]), the (logarithmic) law of the wall is taken basically as an empirical observation rather than a consequence of matching inner and outer layers, as the latter is not felt rich enough to provide a stringent foundation of this important relationship reflecting the dynamics of the flow close to the wall, which is not understood in full at present. Probably the first successful model that describes essential aspects of this dynamics is provided by Prandtl's mixing length concept, proposed more than 50 years before the advent of asymptotic theories in fluid mechanics. Significant progress has been achieved in more recent years and, in particular, by the pioneering work of Walker (e.g. [30]), whose untimely death ended a line of thought which certainly ought to be taken up again.

Following the brief outline of the classical small-defect theory, it is shown how a description of turbulent boundary layers having a slightly larger (i.e. moderately large) velocity defect, where the outer predominately inviscid layer starts to develop a wake-type behaviour, can be formulated. Further increase of the velocity defect to values of $O(1)$ causes the wake region to become even more pronounced and is seen to allow for the occurrence of reverse-flow regions close to the wall, resulting in what we believe to be the first fully self-consistent theory of marginally separated turbulent flows.

Unfortunately, however, this success seemingly does not shed light on the phenomenon of global or gross separation associated with flows past (more-or-less) blunt bodies or, to put it more precisely, flows which start at a stagnation point rather than a sharp leading edge. Indeed, a recent careful numerical investigation for the canonical case of a circular cylinder, presented, among others, in [22, 23], undoubtedly indicates that the boundary layer approaching separation exhibits a small rather than a large velocity defect, leading in turn to the dilemma addressed in Subsect. 2.4. The accompanying asymptotic analysis based on the turbulence intensity gauge model introduced in [15], however, strongly suggests that a boundary layer forming on a body of finite extent and originating in a front stagnation point does not reach a fully de-

veloped turbulent state, even in the limit $Re \to \infty$. Specifically, it is found that the boundary layer thickness and the Reynolds shear stress are slightly smaller than predicted by classical small-defect theory, while, most important, the thickness of the wall layer and possibly the velocity defect in the outer region are slightly larger. As a consequence, the outer large-momentum region does not penetrate to distances from the wall which are transcendentally small. In turn, this situation opens the possibility to formulate a local interaction mechanism that describes the detachment of the boundary layer from the solid wall within the framework of free-streamline theory at pressure levels which are compatible with experimental observation. This is a topic of intense current investigations.

References

1. N. Afzal. Scaling of Power Law Velocity Profile in Wall-Bounded Turbulent Shear Flows. Meeting paper 2005-109, AIAA, 2005.
2. G. I. Barenblatt and A. J. Chorin. A note on the intermediate region in turbulent boundary layers. *Phys. Fluids*, 12(9):2159–2161, 2000. Letter.
3. G. I. Barenblatt, A. J. Chorin, and V. M. Prototoskin. Self-similar intermediate structures in turbulent boundary layers at large Reynolds numbers. *J. Fluid Mech.*, 410:263–283, 2000.
4. G. I. Barenblatt and N. Goldenfeld. Does fully developed turbulence exist? Reynolds number independence versus asymptotic covariance. *Phys. Fluids*, 7(12):3078–3082, 1995.
5. W. B. Bush and F. E. Fendell. Asymptotic analysis of turbulent channel and boundary-layer flow. *J. Fluid Mech.*, 56(4):657–681, 1972.
6. F. H. Clauser. The Turbulent Boundary Layer. In H. L. Dryden and Th. von Kármán, editors, *Advances in Applied Mechanics*, volume 4, pages 1–51. Academic Press, New York, 1956.
7. E. Deriat and J.-P. Guiraud. On the asymptotic description of turbulent boundary layers. *J. Theor. Appl. Mech.*, 109–140, 1986. Special Issue on Asymptotic Modelling of Fluid Flows. Original French article in *J. Méc. Théor. Appl.*
8. F. E. Fendell. Singular Perturbation and Turbulent Shear Flow near Walls. *J. Astronaut. Sci.*, 20(11):129–165, 1972.
9. P. S. Klebanoff. Characteristics of turbulence in a boundary layer with zero pressure gradient. NACA Report 1247, NASA – Langley Research Center, Hampton, VA, 1955. See also NACA Technical Note 3178, 1954.
10. G. L. Mellor. The Large Reynolds Number, Asymptotic Theory of Turbulent Boundary Layers. *Int. J. Engng Sci.*, 10(10):851–873, 1972.
11. G. L. Mellor and D. M. Gibson. Equilibrium turbulent boundary layers. *J. Fluid Mech.*, 24(2):225–253, 1966.
12. R. E. Melnik. An Asymptotic Theory of Turbulent Separation. *Computers & Fluids*, 17(1):165–184, 1989.
13. R. Michel, C. Quémard, and R. Durant. Hypothesis on the mixing length and application to the calculation of the turbulent boundary layers. In S. J. Kline, M. V. Morkovin, G. Sovran, and D. J. Cockrell, editors, *Proceedings of Computation of Turbulent Boundary Layers – 1968 AFOSR-IFP-Stanford Conference*, volume 1, pages 195–207. Stanford University, CA, 1969.

14. P. A. Monkewitz, K. A. Chauhan, and H. M. Nagib. Self-consistent high-Reynolds-number asymptotics for zero-pressure-gradient turbulent boundary layers. *Phys. Fluids*, 19(11):115101-1–115101-12, 2007.
15. A. Neish and F. T. Smith. On turbulent separation in the flow past a bluff body. *J. Fluid Mech.*, 241:443–467, August 1992.
16. J. M. Österlund, A. V. Johansson, H. M. Nagib, and M. Hites. A note on the overlap region in turbulent boundary layers. *Phys. Fluids*, 12(1):1–4, 2000. Letter.
17. A. I. Ruban. Singular Solutions of the Boundary Layer Equations Which Can Be Extended Continuously Through the Point of Zero Surface Friction. *Fluid Dyn.*, 16(6):835–843, 1981. Original Russian article in *Izvestiya Akademii Nauk SSSR, Mekhanika Zhidkosti i Gaza* (6), 42–52, 1981.
18. A. I. Ruban. Asymptotic Theory of Short Separation Regions on the Leading Edge of a Slender Airfoil. *Fluid Dyn.*, 17(1):33–41, 1982. Original Russian article in *Izvestiya Akademii Nauk SSSR, Mekhanika Zhidkosti i Gaza* (1), 42–51, 1982.
19. B. Scheichl and A. Kluwick. On turbulent marginal boundary layer separation: how the half-power law supersedes the logarithmic law of the wall. *Int. J. Computing Science and Mathematics (IJCSM)*, 1(2/3/4):343–359, 2007. Special Issue on Problems Exhibiting Boundary and Interior Layers.
20. B. Scheichl and A. Kluwick. Turbulent Marginal Separation and the Turbulent Goldstein Problem. *AIAA J.*, 45(1):20–36, 2007. See also *AIAA Meeting paper 2005-4936*.
21. B. Scheichl and A. Kluwick. Asymptotic theory of bluff-body separation: a novel shear-layer scaling deduced from an investigation of the unsteady motion. *J. Fluids Struct.*, 24(8):1326–1338, December 2008. Special Issue on the IUTAM Symposium on Separated Flows and their Control.
22. B. Scheichl, A. Kluwick, and M. Alletto. "How turbulent" is the boundary layer separating from a bluff body for arbitrarily large Reynolds numbers? *Acta Mech.*, 201(1–4):131–151, 2008. Special Issue dedicated to Professor Wilhelm Schneider on the occasion of his 70th birthday.
23. B. Scheichl and A. Kluwick. Level of Turbulence Intensities Associated with Bluff-Body Separation for Large Values of the Reynolds number. Meeting paper 2008-4348, AIAA, 2008.
24. H. Schlichting and K. Gersten. *Boundary-Layer Theory*. Springer-Verlag, Berlin, Heidelberg, New York, 8th edition, 2000.
25. W. Schneider. Boundary-layer theory of free turbulent shear flows. *Z. Flugwiss. Weltraumforsch. (J. Flight Sci. Space Res.)*, 15(3):143–158, 1991.
26. K. Stewartson. Multistructured Boundary Layers on Flat Plates and Related Bodies. In Y. Chia-Sun, editor, *Advances in Applied Mechanics*, volume 14, pages 145–239. Academic Press, New York, San Francisco, London, 1974.
27. K. Stewartson, F. T. Smith, and K. Kaups. Marginal Separation. *Studies in Applied Mathematics*, 67(1):45–61, 1982.
28. R. I. Sykes. An asymptotic theory of incompressible turbulent boundary-layer flow over a small hump. *J. Fluid Mech.*, 101(3):631–646, 1980.
29. A. A. Townsend. Equilibrium layers and wall turbulence. *J. Fluid Mech.*, 11(1):97–120, 1961.
30. J. D. A. Walker. Turbulent Boundary Layers II: Further Developments. In A. Kluwick, editor, *Recent Advances in Boundary Layer Theory*, volume 390 of CISM Courses and Lectures, pages 145–230. Springer-Verlag, Vienna, New York, 1998.

31. K. S. Yajnik. Asymptotic theory of turbulent shear flows. *J. Fluid Mech.*, 42(2):411–427, 1970.